Inorganic Chemistry

ARTICLE

pubs.acs.org/IC

Cobalt Complexes with "Click"-Derived Functional Tripodal Ligands: Spin Crossover and Coordination Ambivalence

David Schweinfurth,[†] Fritz Weisser,[†] Denis Bubrin,[†] Lapo Bogani,[*,‡] and Biprajit Sarkar[*,†]

[†]Institut für Anorganische Chemie, Universität Stuttgart, Pfaffenwaldring 55, D-70550, Stuttgart, Germany

[‡]Physikalisches Institut, Universität Stuttgart, Pfaffenwaldring 57, D-70550, Stuttgart, Germany

Supporting Information

ABSTRACT: We demonstrate the use of a Cu(I) catalyzed "Click" reaction in the synthesis of novel ligands for spin crossover complexes. The reaction between azides and alkynes was used to synthesize the reported tripodal ligand tris[(1-benzyl-1*H*-1,2,3-triazol-4-yl)methyl]amine, TBTA, and the new ligands tris[(1-cyclohexyl-1*H*-1,2,3-triazol-4-yl)methyl]amine, TCTA, and tris[(1-*n*-butyl-1*H*-1,2,3-triazol-4-yl)methyl]amine, TBuTA. Reactions of TBTA with $Co(ClO_4)_2$ lead to complexes of the form $[Co(TBTA)(CH_3CN)_3](ClO_4)_2$, **1**, and $[Co(TBTA)_2](ClO_4)_2$, **2**, where complex formation can be controlled by the metal/ligand ratio and the complexes **1** and **2** can be chemically and reversibly switched from one form to another in solution resulting in coordination ambivalence. The benzyl substituents of TBTA in **2** show intramolecular C−H—π T-stacking that generates a chemical pressure to stabilize the low spin (LS) state at lower temperatures. The structural parameters of **2** are consistent with a Jahn−Teller active LS Co(II) (elongation) ion showing four short and two long bonds. **2** shows spin-crossover (SCO) behavior in the solid state and in solution with a high T_0 close to room temperature which is driven by the T-stacking. **1** remains high spin (HS) between 2 and 400 K. Reversible chemical switching is observed between **1** and **2** at room temperature, with an accompanying change in the spin state from HS to LS. The importance of the intramolecular T-stacking in driving the SCO behavior is proven by comparison with two analogous compounds that lack an aromatic substituent and remain HS down to very low temperatures.

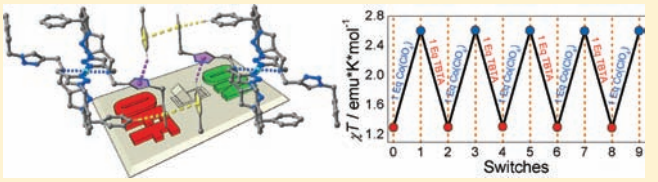

INTRODUCTION

The 1,3-dipolar cycloaddition reaction between alkynes and azides was reported by Huisgen et al. decades ago.[1] The Cu-catalyzed version of this reaction, recently reported by two independent groups, and now known as the "Click" reaction, has many advantages compared to the noncatalyzed form.[2] The catalyzed version leads selectively to only one regioisomer of the triazole, works under mild conditions in environmentally benign solvents, and the work up steps are simpler. The above-mentioned points, together with the excellent functional group tolerance of this reaction, have recently made it one of the most important tools in synthetic strategies. Since the initial discovery of the "Click reaction", this method has found use in areas of chemistry as diverse as dendrimers and polymers,[3] drug discovery,[4] material science,[5] bioconjugation,[6] and metal responsive flourophores,[7] just to name a few. Anyway, its use and advantages in the creation of functional ligands for magnetically bistable metal complexes is still largely unexplored.[8] This is surprising because of the advantages that this approach has to offer: "click reactions" now allow using tripodal ligands with 1,2,3-triazole rings with a large choice of functional groups perfectly arranged in the desired geometry. The freedom of choice of the appendages also allows studying in detail the effects of weak interactions like π or T-stacking (Scheme 1), both intramolecular and intermolecular.

Such characteristics are particularly useful for metal complexes that can undergo transitions from one state to another, like spin-crossover (SCO) compounds. Metal centers with an electronic configuration of d^{4-7} in an octahedral ligand field can exist either in the high spin (HS) or low spin (LS) forms, depending on the ligand field stabilization and spin pairing energies. SCOs are characterized by the fact that the spin ground state changes with temperature T, from HS to LS, leading to a characteristic variation of the magnetic behavior around a transition temperature T_0.[9] Light is also a frequently used as external stimulus to induce such transitions.[10] Reversible photoinduced spin state switching has recently been observed for d^8 metal centers as well[11] and iron complexes are well-known for showing SCO.[12] Certain Co(II) complexes also undergo SCO, but the energy range in which SCO is observed is much narrower than their iron counterparts, thus requiring fine-tuning of the electronic states.[13a,b] The majority of octahedral Co(II) SCO complexes are based on the terpyridine ligands which impose a tetragonal compression in the Jahn−Teller active d^7, LS Co(II) center. Examples of SCO in Co(II) complexes where a tetragonal elongation is observed in the LS form are also known. In most of these cases it is the ligand rigidity that provides the high enthalpic barrier required for SCO.[13,14] Ligands produced with the click chemistry approach might provide possibilities for weak interactions that could then drive the SCO in relevant systems.

In the following we present the first use of Click-derived 1,2,3-triazole tripods for SCOs and the creation of four new Co(II)

Received: February 4, 2011
Published: June 09, 2011

Scheme 1. Structures of the 1,2,3-Triazoles Ligands Used and of the Allowed Conformational Freedom[a]

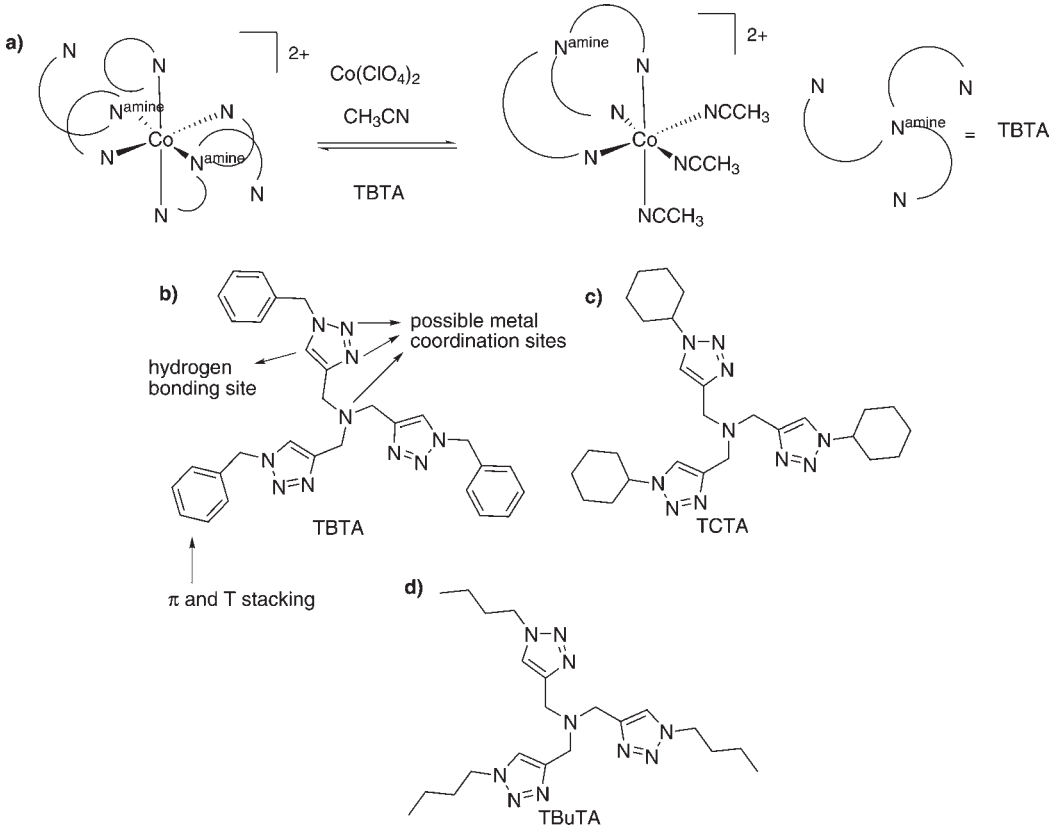

[a] (a) Scheme of the reversible chemical transformation between Co(II) complexes **1** and **2**. (b) TBTA ligand; (c) TCTA ligand; (d) TBuTA ligand.

complexes. The effect of soft-donor click ligands on the magnetic states of Co(II) systems is investigated, showing the presence of SCO behavior at high temperatures. The enhanced structural and chemical flexibility is then exploited to investigate the role of the functional groups and different coordination modes. The use of click reaction allows substituting the functionalities with different ones, clearly showing the effect of intra- and intermolecular stacking interactions. Eventually the enhanced properties of the ligands are highlighted by the possibility of having, at the same time, coordination ambivalence, high SCO temperatures, and sufficient flexibility for a reversible ligand exchange, reversibly switching the system from the HS to the LS state in solution.

RESULTS AND DISCUSSION

Ligand Design and Synthesis. Targeted ligand design is at the heart of generating SCO metal complexes. Tuning of the steric and electronic properties (including weak interactions) of ligands is fundamental for the creation of SCO compounds with high transition temperatures and thermal hysteresis.[10d,15] Intramolecular interactions that produce a more rigid ligand shell normally induce an increase in the transition enthalpy, thus raising T_0. Intermolecular interactions, which give rise to cooperative effects, can produce thermal hysteresis in the SCO behavior.

Up to now the strategy to obtain high transition temperatures has relied on the use of very rigid cages and ligands that strongly bind onto the metal center. Fe-based SCO compounds are mostly based on rather rigid ligands with N-containing coordinating groups. Co-based SCO materials are relatively less investigated, and most of the systems considered use strong donors based on P, diimine, or rigid terpyridine ligands.[13]

Here we pursue a different strategy, made possible by the use of click-derived ligands, using 1,2,3-triazole tripods. Such ligands have more binding modes and a larger structural flexibility than the widely investigated terpyridine ligands, thus allowing for easier ligand exchange. The N2 and N3 atoms of triazole ligands (Scheme 1) can bind to metal centers, and their differing basicities can be used for selective metal coordination. The relatively high acidity of the ring C−H proton of the 1,2,3-triazoles makes this an ideal candidate to generate hydrogen bonding networks, and this strategy has been extensively used for anion binding with 1,2,3-triazoles as anion receptors.[16] The use of 1,4-substituted 1,2,3-triazoles as ligands in coordination chemistry has seen a recent surge,[17] and for SCOs this can provide additional opportunities for metal coordination, hydrogen bond formation, and stacking interactions. N2 and N3 can also be used for generating weak interactions. In this work we show the importance of such functional sites in the creation of SCO compounds using these ligands. The enhanced flexibility of these ligands allows coordinating the metal ion in different ways, contrarily to previously used systems. This should lead to the possibility of reversibly changing the coordination environment of the metal center (Scheme 1a).

The ligand we chose is the tripodal ligand tris[(1-benzyl-1*H*-1,2,3-triazol-4-yl)methyl]amine, TBTA (literature known, Scheme 1b), which provides additional coordination possibilities through the central amine nitrogen and multiple sites for generating weak interactions. The synthetic path used (Experimental Section) is described in Scheme 2.

dx.doi.org/10.1021/ic200246v |*Inorg. Chem.* 2011, 50, 6114–6121

Scheme 2. Synthesis of the Tripodal Click Ligands

Table 1

	compound		
	1	**2**	**3**
chemical formula	$C_{36}H_{39}N_{13}Co \cdot C_2H_3N.2(ClO_4)$	$C_{60}H_{60}N_{20}Co.2(ClO_4)$	$C_{54}H_{84}N_{20}Co.2(ClO_4)$
M_r	952.69	1319.11	1271.4
crystal system, space group	triclinic, $P\bar{1}$	triclinic, $P\bar{1}$	orthorhombic, *Pbca*
temperature (K)	173	173	100
a, *b*, *c* (Å)	12.405(2), 12.482(2), 17.162(3)	10.182(2), 11.401(2), 13.982(2)	17.990(1), 18.387(2), 18.396(1)
α,β,γ (deg)	79.928(14), 78.168(11), 60.612(13)	94.385(11), 104.667(9), 93.441(12)	90, 90, 90
V (Å^3)	2257.5(7)	1560.4(4)	6085.30(16)
Z	2	1	4
density (g/cm^3)	1.402	1.404	1.388
F(000)	986	685	2692
radiation type	Mo *K*α	Mo *K*α	Mo *K*α
μ (mm^{-1})	0.7107	0.7107	0.7107
crystal size (mm)	0.5× 0.45 × 0.2	0.55× 0.3 × 0.2	0.1× 0.09× 0.09
meas., indep. and obsvd [$I > 2\sigma(I)$] refl.	9047, 8625, 6495	7538, 7137, 5042	14056, 7367, 5684
R_{int}	0.0357	0.0398	0.0276
$R[F^2 > 2\sigma(F^2)]$, $wR(F^2)$, *S*	0.051, 0.1398, 0.963	0.0453, 0.1243, 0.917	0.0503, 0.1153, 1.079
$\Delta\rho_{max}$, $\Delta\rho_{min}$ (e Å^{-3})	0.771, −0.604	0.633, −0.438	0.696, −0.619

The ligands TCTA and TBuTA (Schemes 1c and 1d) were also synthesized (Experimental Section) by the copper catalyzed Click reaction between tris-propargyl amine and cyclohexyl azide or *n*-butyl azide respectively. These ligands possess no aromatic substituents, so that π- and T-stacking interactions should be suppressed, both within the molecule and among molecules. This allows investigating the importance of the interactions in 1,2,3-triazole-based SCO compounds.

Synthesis and Structure of the Complexes. Reactions of $Co(ClO_4)_2 \cdot 6H_2O$ with equimolar amounts of TBTA at room temperature resulted in the formation of $[Co(TBTA)(CH_3CN)_3](ClO_4)_2$, **1**. An analogous procedure afforded $[Co(TCTA)_2](ClO4)_2$, **3**, or $[Co(TBuTA)_2](ClO4)_2$, **4**, by reacting $Co(ClO4)_2 \cdot 6H_2O$ with 2 equiv of TCTA or TBuTA, respectively. Compound $[Co(TBTA)_2](ClO_4)_2$, **2**, could be prepared by two different procedures. Reaction of 1 equiv of $Co(ClO4)_2 \cdot 6H_2O$ with 2 equiv of TBTA led to the formation of **2**. Alternatively, the addition of 1 equiv of TBTA to **1** leads to the formation of **2** through the substitution of the three labile acetonitrile ligands. One of the TBTA ligands of **2** can be substituted back by acetonitrile molecules by the addition of $Co(ClO_4)_2 \cdot 6H_2O$ which gives back **1** (Scheme 1a). It is to be noticed that similar procedures are not possible for most Fe complexes that have high T_0 temperatures. Here, on the contrary, the different coordination modes allowed by the enhanced flexibility of the ligand can be switched back and forth, demonstrating the flexibility and advantages of this approach.

Complexes **1**−**3** could be obtained as single crystals suited for X-ray inspection. Compounds **1** and **2** were crystallized by slow diffusion of diethylether into acetonitrile solutions, while **3** crystallized upon slow cooling of the methanol solution. Measurements at 173 K showed that both **1** and **2** crystallize in the triclinic $P\bar{1}$ space group, whereas **3** crystallizes in the orthorhombic *Pbca* space group. Crystallographic details are given in Table 1.

The cobalt center in compound **1** (Figure 1) is coordinated by the nitrogen atoms of the three triazole rings of TBTA with average Co−N distances of 215 ± 1 pm. Three other positions are occupied by acetonitrile molecules positioned at 222 ± 1, 224 ± 2, and 250 ± 1 pm from the Co center. There is a seventh coordination to the central amine nitrogen of TBTA which is at a distance of 265 ± 1 pm from the Co center. The capping bond is longer than the others, but consistent with other heptacoordinate complexes and also significantly shorter than what is expected for noncoordinating nitrogens (about 280 pm for Co(II)-N(amine).[18] To our knowledge this is the first example of such coordination geometry with Co(II) complexes using tetradentate tripodal ligands. This shall be ascribed to the coordination flexibility that these ligands bring with them. The resulting capped octahedron shows that the CH_3CN molecules are placed in an almost perfect triangular structure (Supporting Information, Figure S1), as well as the three triazoles. The coordination around the cobalt center in **1** is thus that of a rare cappedoctahedron with Co−N distances typical of a HS Co(II)

dx.doi.org/10.1021/ic200246v |*Inorg. Chem.* 2011, 50, 6114–6121

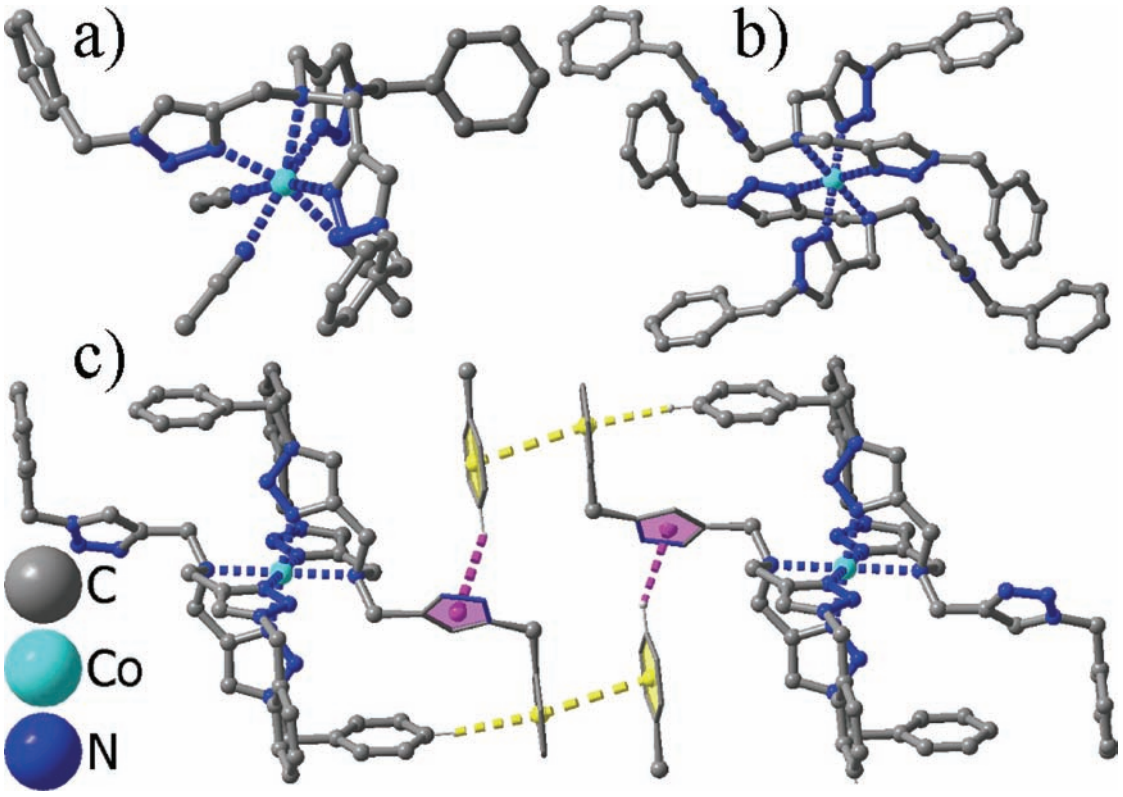

Figure 1. Structures of the compounds, with hydrogens and counterions omitted for clarity. Coordination bonds and stacking interactions are represented as fragmented. (a) Structure of **1**, showing the heptacoordinate Co(II) center. (b) Structure of **2**, showing the disposition of the two binding arms of TBTA and the nonbinding one. (c) View of the intramolecular and intermolecular stacking interactions. Only two molecules of **2** and the benzyl rings of adjacent molecules are represented. The involved benzyl rings and centroids are yellow, the triazoles purple, and the relevant H atoms white.

center.[13a] There are no significant intermolecular interactions in case of **1**, the only significant weak interaction being that between the C−H of the triazole rings and the perchlorate ions. Such C−H···anion interactions have been made use of as using triazole containing molecules as anion receptors.[16]

In contrast, the cobalt center in **2** is coordinated by two TBTA ligands resulting in hexacoordination with complete absence of acetonitrile molecules (Figure 1). Each TBTA binds to the cobalt center through two of the triazole nitrogen atoms at relatively short Co−N distances of 193 ± 1 pm. These four triazole nitrogen thus occupy the equatorial positions of the octahedron. The axial positions are occupied by the amine nitrogen atoms of each TBTA, and the Co−N distance here is 236 ± 1 pm. The resulting geometry is an axially elongated octahedron, as expected for a LS Jahn−Teller distorted Co(II) center, in which one triazole arm of TBTA is left noncoordinating.[13a]

This remaining arm allows the formation of a rather complex pattern of stacking interactions, both intramolecular and intermolecular (Figure 1). The benzyl ring of one of the coordinating arms forms two intermolecular interactions with two adjacent molecules. One is a T-stacking between one of the benzyl hydrogens and the 1,2,3-triazole ring of the uncoordinating arm of an adjacent molecule (H-ring center distance of 280 ± 1 pm). The other interaction is a weak π-stacking (planes distance of 380 ± 1 pm at an angle of 11°) with the benzyl appendage of another adjacent molecule. This latter benzyl ring is further T-stacked in an intramolecular fashion with the hydrogen atom (H-ring center distance of 269 ± 4 pm) of a coordinating arm of the other TBTA ligand. The resulting pattern helps stabilize the

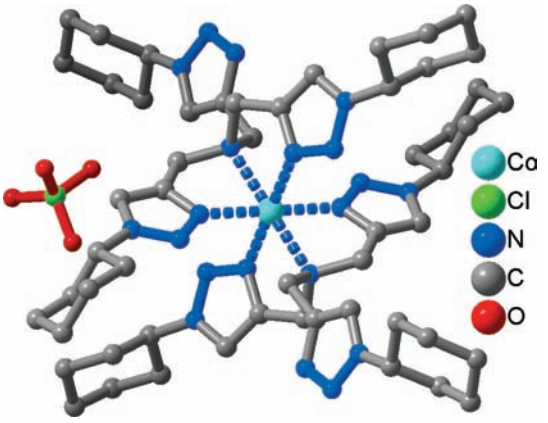

Figure 2. View of the molecular structure for **3**. Average Co−N(triazole) distances = 210 ± 1 pm and average Co−N(amine) distance = 225 ± 1 pm.

complex and make it more rigid but, at the same time, it does not hinder the internal flexibility. The ligand allows different coordination geometries and coordination ambivalence, as shown by **1** and **2**. The arrangements of molecules are also completely different, with **1** showing no significant intra- or intermolecular weak interactions whereas **2** engage in such interactions as discussed above.

The cobalt center in **3** is coordinated by two TCTA molecules, in a manner similar to **2** (Figure 2). However, the average Co−N(triazole) distances of 210 ± 1 pm are longer than the corresponding distances in **2**, and the average Co−N(amine) distances of 225 ± 1

dx.doi.org/10.1021/ic200246v |*Inorg. Chem.* 2011, 50, 6114–6121

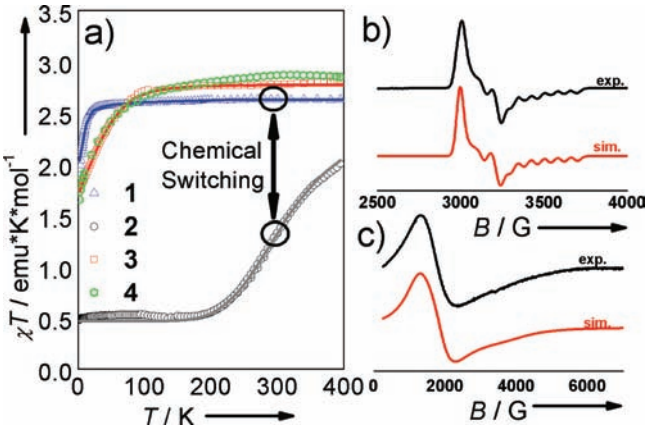

Figure 3. Magnetic properties of the compounds. (a) Temperature dependence of the χT value for **1** (red triangles), **2** (black circles), **3** (blue squares), and **4** (green pentagons) in the 2−400K range. Lines are fits to the data (see text). The chemical switching equilibrium is highlighted. (b) X-band EPR spectra of **1**, f = 9.6727, and (c) of **2**, f = 9.6726, as polycrystalline powder acquired at 110 K, together with the corresponding simulations (see text).

pm are shorter than the corresponding distances in **2**. There are also no significant noncovalent interactions observed for **3** as is the case for **2**. The Co−N distances in **3** are compatible with those of a HS Co(II) center. Like **1**, **3** also do not show any significant intermolecular interactions other than the C−H (triazole)···ClO_4^- interactions as in the case of **1**.

The uncoordinated triazole arms of the TBTA ligands in **2** participate in intra- and intermolecular noncovalent interactions. In particular, the intramolecular T-stacking between the benzyl substituents of different triazole rings creates a chemical pressure within the molecule which results in a LS Co(II) state for **2** at lower temperature as seen from the Co−N bond lengths as well as SQUID and electron paramagnetic resonance (EPR) spectroscopic measurements (see discussion below). Such interactions are missing in **1** and hence the Co(II) center in **1** is in the HS state even at low temperatures. That such interactions are important for generating a chemical pressure and hence altering the spin state of the Co(II) center is proven by the properties of complex **3**. This compound is analogous to **2** but lacks the possibilities of a T-stacking since the cyclohexyl rings are not aromatic. Thus, in spite of having the same first coordination sphere as **2**, **3** shows bond lengths and magnetic properties that are typical of a HS Co(II) center.

Magnetic Behavior. The magnetic properties of the samples of **1**, **2**, **3**, and **4** were investigated with a SQUID magnetometer in the 2−400 K temperature (T) range. The T dependence of the χT product, where χ is the molar static magnetic susceptibility, defined as the ratio between the molar magnetization and the applied magnetic field, is reported in Figure 3a for all compounds. **1** shows a room temperature χT value of about 2.6 emu K/mol, in good agreement with the reported values for an isolated, HS Co(II) center,[13] with spin state S = 3/2 (ground state $^4T_{1g}$). χT remains constant down to 23 K, where the effect of depopulation of the higher Kramers levels becomes appreciable and χT then decreases to 2.0 emu K/mol at 2 K. The behavior could be fitted by considering a zero-field splitting of the spin ground state S = 3/2 with the Hamiltonian $\mathscr{H} = D[S_z^2 - S(S+1)/3] + \mathbf{HgS}/k_BT$, where S_z is the z-component of the spin and k_B is the Boltzmann constant, affording $|D|$ = 8.2 cm^{-1}. Addition of intermolecular interactions did not improve the fit.

On the contrary, **2** shows a very sharp decrease of the χT value from 2.0 emu K/mol at 400 K to 1.3 emu K/mol at 300 K to reach a constant value of 0.47 emu K/mol below 150 K, which agrees well with a LS Co(II) center.[13] (Figure 3a) The observed behavior is quite typical of SCO compounds, and indicates a high T_0, comparable to those obtained with the very rigid terpyridine ligands. The regular solution model describes well the data by

$$\chi T = \chi_{LS}T + (\chi_{HS}T - \chi_{LS}T)\eta_{HS} \quad (1)$$

where χ_{LS} = 0.5 emu K/mol and χ_{HS} = 2.5 emu K/mol correspond to the LS and HS susceptibilities, respectively, and η_{HS} is the HS molar fraction at a given T. η_{HS} is related to the thermodynamic quantities governing the transition by $\ln(1 - \eta_{HS}/\eta_{HS}) = [\Delta H - T\Delta S - \Gamma(1-2\eta_{HS})]/RT$, where ΔH and ΔS are the enthalpy and entropy variations, R is the universal gas constant, and Γ accounts for cooperative effects. Solution of the transcendental equation with graphical methods (Supporting Information, Figure S3 and S4) and least-squares fitting (agreement R^2 = 0.9995) leads to ΔH = 13.9 ± 0.2 kJ/mol, ΔS = 43 ± 1 J K^{-1} mol^{-1}, Γ = 0.4 kJ/mol. This corresponds to η_{HS} = 0.4 at 300 K. ΔH and ΔS values are appreciably higher to those found for more rigid ligands in Co-based SCOs.[13] In particular the ΔS value is larger than expected for the spin change of a Co(II) ion, 5.8 J K^{-1} mol^{-1}. The remainder entropy should be assigned to vibrational and conformational changes in the molecule, made easier by the TBTA ligand. The very high ΔH value that drives T_0 toward room temperature cannot be justified by a structural rigidity of the ligand, as in studies of terpyridine based complexes, and shall rather be justified by the presence of the intramolecular T-stacking interaction, whose energy scale is of the order of tens of kJ/mol.[19] The Γ factor is much smaller than $2RT_0$, and thus no thermal hysteresis is observed, consistent with the lack of hydrogen bonds and the presence of weaker stacking interactions.

The importance of the stacking interactions in driving the transition is clearly shown by **3** and **4** whose room temperature χT value (2.9 emu K/mol) remains constant down to 115 K, when χT starts dropping, reaching a value of 1.8 emu K/mol at 2 K (Figure 3a). The behaviors for both compounds are remarkably similar, with the curves almost superimposing one over another. Appreciable effects of the depopulation of Co(II) levels are normally observed below 60 K, and this behavior could be due to zero field splitting effects. Should it be assigned to a low-temperature SCO effect, fitting of the curve for **3** with eq 1 (R^2 = 0.9995), yields ΔH = 1.0 ± 0.5 kJ/mol, ΔS = 15 ± 3 J K^{-1} mol^{-1}, Γ = 0.5 kJ/mol. Whatever the case the sharp drop of T_0 clearly reveals the importance of the intramolecular interactions in driving the SCO transition. The two ligands have very different steric encumbrances and an expansion of the ligand sphere because of unfavorable intramolecular steric pressure cannot account for the high-spin nature. On the contrary, both compounds cannot lead to stacking interactions, as they lack aromatic substituents.

EPR Spectroscopy. The X-band EPR spectra of **1**, **2**, **3**, and **4** recorded at 110 K as a polycrystalline powder (Figure 3 and Supporting Information, Figure S5) show the presence of a HS state for **1**, **3**, and **4** and LS state for **2**, consistently with the magnetization data. The spectra could be simulated with g-values of 5.35, 3.65, and 1.87 for **1** and 5.60, 3.70, and 2.10 for **3**. This leads to a g_{av} value of the high spin system of 3.62 and 3.80

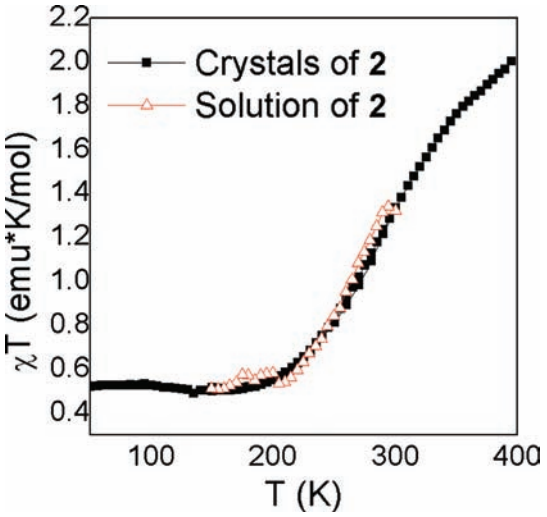

Figure 4. Magnetic characterization of **2** in solid state and in solution. Temperature dependence of the χT value for microcrystals of **2** (black squares) and for a solution of **2** in CH_3CN. The diamagnetic contribution from the solution and sample holder was subtracted.

respectively. The extremely broad signal for **4** precluded a reasonable simulation and g value determination for this compound. The LS complex **2** could be simulated with $g_\perp = 2.221$ ($A_\perp = 30$G) and $g_\parallel = 2.020$ ($A_\parallel = 80$G). Compounds **1**, **3**, and **4** which are in the HS state show broad EPR lines because of fast relaxation processes owing to high spin−orbit coupling associated with HS Co(II) centers.[19e,20] **4** (Supporting Information, Figure S5) shows much broader lines compared to **1** and **3**, and this probably indicates the influence of the *n*-butyl substituents in **4** in enhancing the relaxation phenomenon.

These EPR data corroborate the susceptibility measurements. **1**, **3**, and **4** show EPR spectra at 110 K that are typical of a HS Co(II) center. The transition observed in this case arises from the low-lying $S = 1/2$ manifold. Transitions related to the $S = 3/2$ state are usually not observed in the X-band because of the large zero field splitting associated with a HS Co(II) centers. The broad lines and large g-anisotropy are an indication of fast relaxation processes as is brought about by the large spin−orbit coupling of the HS Co(II) centers. **2** shows a much narrower EPR signal than **1** and **3** because of the slower relaxation times of the LS Co(II) center of **2**. The narrower lines also result in the resolution of the hyperfine coupling to the ^{59}Co nucleus, which has a nuclear spin, $I = 7/2$.

Reversible Switching Behavior. A reversible chemical switching is possible between **1** and **2** in solution, as shown in Scheme 1. The complex formation can be controlled by metal/ligand ratio and the complexes **1** and **2** can be reversibly switched from one form to another in solution, resulting in coordination ambivalence. Structural characterization at 173 K shows Co−N distances for **1** that are typical for a high spin Co(II) complex. In contrast, **2** shows Co−N distances typical for a Jahn−Teller distorted low spin Co(II) center with TBTA coordinating through two of the triazole nitrogens and central amine nitrogen atom with one triazole arm being free. The benzyl substituents of the free triazole arms of **2** participate in intramolecular C−H---π T-stacking that generates a chemical pressure to stabilize the LS state at lower temperatures. **2** shows SCO behavior in the solid state and in solution, as probed by SQUID susceptometry, with a high T_0 close to room temperature which is driven by the T-stacking. **1** remains HS between 2 and 400 K. The chemical switching between **1** and **2** in solution is accompanied by a complete switching of the spin state of Co(II) (Figure 4). This result accompanied by the fact that **2** shows SCO behavior in solution suggests the importance of weak intramolecular interactions in driving such processes. The switching between **1** and **2** is also accompanied by a color change as seen from differences in their absorption spectra (Supporting Information, Figure S6).

CONCLUSIONS

Click-chemistry allows for an enormous enrichment of the variety of triazole ligands, and an unprecedented rational tuning of the groups, and opens up new possibilities for generating ligands for bistable complexes as mentioned above. **2** shows SCO behavior with a high T_0. Reversible chemical switching is observed between **1** and **2** at room temperature with an accompanying change in the spin state from HS to LS. The importance of the intramolecular T-stacking in driving the SCO behavior is proven by the magnetic properties of $[Co(TCTA)_2](ClO4)_2$, **3**, and $[Co(TBuTA)_2](ClO4)_2$, **4**, which are analogous to **2** but lack an aromatic substituent and remain HS until low temperatures. On the other hand, the SCO behavior of **2** is maintained in the solid state as well as in solution. We have created a new Co(II) complex in which the structural flexibility of the ligand is assisted by internal T-stacking interactions in creating a room-temperature SCO transition. Unlike the more rigid terpyridine ligands, the magnetic properties of these complexes can be chemically switched in a fully reversible way. The structural flexibility of the ligands allows for a change in their coordination mode hence making them coordination ambivalent. These results afford insights into the role of different interactions in SCOs and highlight the unexplored potential of increasingly popular "Click-based" ligands in the chemistry of Co(II) complexes and for magnetic bistability.

EXPERIMENTAL SECTION

General Procedures and Materials. All manipulations were carried out under air. Tripropargylamine and $Co(ClO_4)_2 \cdot 6H_2O$ were purchased from Sigma Aldrich and used as received. TBTA and cyclohexylazide were prepared according to the literature procedures.[21] ***Caution!*** *Perchlorate salts of metal complexes with organic ligands are potentially explosive. Heating of dried samples must be avoided; handling of small amounts has to proceed with great caution using protection.*

Synthesis of Tris[(1-cyclohexyl-1*H*-1,2,3-triazole-4-yl)methyl]amine (TCTA). Cyclohexylazide, 2.86 g (22.9 mmol), and tripropargylamine, 1.00 g (7.62 mmol), were dissolved in a mixture of $CH_2Cl_2/H_2O/$*tert*-butanol (25 mL/25 mL/50 mL). $CuSO_4 \cdot 5H_2O$, 0.286 g (1.14 mmol), sodium ascorbate, 0.905 g (4.57 mmol), and TBTA, 0.121 g (0.23 mmol), were added, and the solution was stirred for 5 days at 50 °C. The reaction mixture was poured into water (100 mL) and was extracted with CH_2Cl_2 (3·50 mL). The combined organic layers were washed several times with water (3·50 mL), dried over Na_2SO_4, and the solvent was evaporated. The product was recrystallized from methanol to yield white crystals (2.51 g, 65%). Anal. Calcd for $C_{27}H_{42}N_{10}$: C, 64.00; H, 8.35; N, 27.64; Found C, 63.88; H, 8.40; 27.62. HRMS (ESI) Calcd for $C_{27}H_{42}N_{10}Na$ ($[M + Na]^+$): m/z 529.3486; found 529.3495. ^{1}H NMR (250 MHz, $CDCl_3$, δppm): 1.30 (m, 3H, cyclohexyl); 1.39−1.52 (m, 6H, cyclohexyl); 1.71−1.83 (m, 9H, cyclohexyl); 1.92 (d, $^3J_{H-H} = 13.6$ Hz, 6H, cyclohexyl); 2.21 (d, $^3J_{H-H} = 13.3$ Hz, 6H, cyclohexyl); 3.77 (s, 6H, NCH_2); 4.43 (t, $^3J_{H-H} = 11.8$ Hz, 3H, cyclohexyl C*H*); 7.79 (s, 3H, 5-triazole-*H*). ^{13}C NMR (100 MHz, $CDCl_3$, δppm): 25.3; 25.3; 33.7; 47.3; 60.2; 121.9; 128.1. The protocols for the click reaction were not optimized, but the formation of three

triazole cycles in one molecule consumes more time than just a regular click reaction.

Tris[(1-*n*-butyl-1*H*-1,2,3-triazole-4-yl)methyl]amine (TBuTA). Butyl iodide (4.51 g, 24.5 mmol) and sodium azide (1.75 g, 30.0 mmol) were dissolved in H_2O/*tert*-butanol (25 mL/50 mL). The solution was refluxed overnight. Then the solution was allowed to cool down, and tripropargylamine (500 mg, 3.82 mmol), $CuSO_4 \cdot 5H_2O$ (143 mg, 0.57 mmol), sodium ascorbate (454 mg, 2.29 mmol), and TBTA (30.4 mg, 0.06 mmol) were added. Afterward the mixture was stirred for additional 5 days at 50 °C. The reaction mixture was poured into water (100 mL) and was extracted with CH_2Cl_2 (3 · 50 mL). Then the combined organic layers were washed several times with water (3 · 50 mL), dried over Na_2SO_4, and the solvent was evaporated. Finally, the compound was cleaned by flash chromatography on silica gel (DCM/MeOH). The product was obtained as a white solid (950 mg) in 58% yields. Anal. Calcd. for $C_{21}H_{36}N_{10}$: C, 58.85; H, 8.47; N, 32.68; Found C, 58.60; H, 8.23; 32.79. HRMS (ESI) Calcd for $C_{21}H_{37}N_{10}$ ($[M + H]^+$): *m*/*z* 429.3197; found 429.3191. ^{1}H NMR (250 MHz, $CDCl_3$): δ 0.95 (t, $^3J_{H-H}$ = 7.3 Hz, 9H, CH_3); 1.36 (sextet, $^3J_{H-H}$ = 7.6 Hz, 6H, CH_2); 1.89 (quintet, $^3J_{H-H}$ = 7.3 Hz, 6H, CH_2); 3.74 (s, 6H, NCH_2); 4.35 (t, $^3J_{H-H}$ = 7.3 Hz, 6H, CH_2); 7.75 (s, 3H, 5-triazole-*H*). ^{13}C NMR (62.5 MHz, $CDCl_3$): δ 13.5; 19.6; 32.4; 47.1; 50.1; 123.8; 143.9.

Preparation of $[Co(TBTA)(CH_3CN)_3](ClO_4)_2$ (1). $Co(ClO_4)_2 \cdot 6H_2O$, 0.366 g (1.00 mmol) was dissolved in 20 mL of CH_3CN. TBTA, 0.531 g (1.00 mmol), was added, and the solution was stirred at room temperature for 2 h. Ten milliliters of diethylether was added, and the product was precipitated by cooling the solution down to −20 °C overnight. The bright pink solid was filtered and washed with diethylether to yield the desired product (0.866 g, 95%). X-ray quality crystals were grown by slow diffusion of ether into an acetonitrile solution. Anal. Calcd for $C_{36}H_{39}Cl_2CoN_{13}O_8$: C, 47.43; H, 4.31; N, 19.97. Found: C, 47.35; H, 4.51; N, 20.04. MS (ESI) Calcd for $C_{30}H_{30}ClCoN_{10}O_4$ ($[M - (ClO_4^-) - 3(CH_3CN)]^+$): *m*/*z* 688.1; Found 688.1. UV−vis (CH_3CN): λ_{max} (ε [M^{-1} cm^{-1}]) 269 nm (17800), 497 nm (87), 536 nm (87), 698 nm (6) ($^4T_1 \rightarrow {}^4T_2$, higher energy bands are metal-to-ligand charge-transfer (MLCT) and IL in origin).

Preparation of $[Co(TBTA)_2](ClO_4)_2$ (2). The compound could be prepared by two alternative procedures and the identity of the product was proven by X-ray crystallography. a) $Co(ClO_4)_2 \cdot 6H_2O$ 0.73.0 g (0.20 mmol) was dissolved in 10 mL of CH_3CN. TBTA, 0.212 g (0.4 mmol) was added and the solution was stirred at room temperature for 2 h. Ten mL of diethylether was added and the product was precipitated by cooling the solution down to −20 °C overnight. The bright pink solid was filtered and washed with diethylether to yield the desired product (0.171 g, 65%). X-ray quality crystals were grown by slow diffusion of diethylether into an acetonitrile solution. b) $[Co(TBTA)(CH_3CN)_3](ClO_4)_2$ 0.130 g (0.14 mmol) and TBTA, 0.074 g (0.14 mmol) were dissolved in 15 mL of CH_3CN. The resulting pink solution was stirred for 2 h at room temperature. Ten mL of diethylether was added and the product was precipitated by cooling the solution down to −20 °C overnight. The light pink solid was filtered and washed with diethylether to yield the desired product (0.148 g, 80%). X-ray quality crystals were grown by slow diffusion of ether into an acetonitrile solution. Anal. Calcd for $C_{60}H_{60}Cl_2CoN_{20}O_8$: C, 54.63; H, 4.58; N, 21.24. Found: C, 54.41; H, 4.62; N, 21.23. MS (ESI) Calcd for $C_{60}H_{60}CoN_{20}$ ($[M - 2(ClO_4^-)]^{2+}$): *m*/*z* 559.7; Found 559.7. UV−vis (CH_3CN): λ_{max} (ε [M^{-1} cm^{-1}]) 265 nm (10800), 481 nm (59) sh, 515 nm (66), 615 nm (48) ($^2E \rightarrow {}^2T_2$, $^2T_1$, higher energy bands are MLCT and IL in origin).

Preparation of $[Co(TCTA)_2](ClO_4)_2$ (3). $Co(ClO_4)_2 \cdot 6H_2O$, 0.050 g (0.14 mmol), and TCTA, 0.142 g (0.28 mmol), were dissolved in 25 mL of methanol, and the solution was refluxed for 1 h. The solution was allowed to cool down overnight, and the product was collected by filtration (0.133 g, 75%) as light pink crystals that allowed for X-ray diffraction. Anal. Calcd for $C_{54}H_{84}Cl_2CoN_{20}O_8$: C, 51.02; H, 6.66; N, 22.04. Found: C, 50.98; H, 6.67; N, 22.10. UV−vis (CH_3CN): λ_{max} (ε [M^{-1} cm^{-1}]) 235 nm (5160), 493 nm (81), 515 nm (84), 610 nm (33) ($^4T_1 \rightarrow {}^4T_2$, higher energy bands are MLCT and IL in origin).

$[Co(TBuTA)_2](ClO_4)_2$ (4). $Co(ClO_4)_2 \cdot 6H_2O$ (42.7 mg, 0.12 mmol) was dissolved in CH_2Cl_2 (5 mL). TBuTA (100 mg, 0.23 mmol) was added, and the solution was stirred at room temperature for 2 h. The solvent was evaporated, and the bright pink solid was dried at high vacuum to yield the desired product (120 mg, 90%). Anal. Calcd. for $C_{42}H_{72}Cl_2CoN_{20}O_8 \cdot CH_2Cl_2$: C, 43.04; H, 6.22; N, 23.35; Found C, 43.15; H, 6.27; 23.10. HRMS (ESI) Calcd for $C_{42}H_{72}CoN_{20}$ ($[M - 2(ClO_4^-)]^{2+}$): *m*/*z* 457.7785; found 457.7791. UV−vis (CH_3CN):λ_{max} (ε [M^{-1} cm^{-1}] 230 nm (5050), 480 nm (90), 520 nm (75), 615 nm (35) ($^4T_1 \rightarrow {}^4T_2$, higher energy bands are MLCT and IL in origin).

Crystallography. Single crystals were grown as mentioned above. A suitable crystal was selected under a layer of viscous hydrocarbon oil, attached to a glass fiber, and instantly placed in a low-temperature N_2-stream. The X-ray intensity data were collected at 173 K using a Siemens P4 diffractometer. Calculations were performed with the SHELXTL PC 5.03 and SHELXL-97 program.[22] The structures were solved by direct methods and refined on F_o^2 by full-matrix least-squares refinement. Anisotropic thermal parameters were included for all non-hydrogen atoms. CCDC 778709−778711 and the Supporting Information contain the cif files of the structures. All these data can be obtained free of charge from the Cambridge Crystallographic Data Centre via www.ccdc.cam.ac.uk/data_requests/cif.

General Instrumentation. ^{1}H NMR spectra were recorded at 250.13 MHz on a Bruker AC250 instrument. X-band EPR spectra were recorded with an EMX Bruker System connected with an ER 4131 VT variable temperature accessory, and simulations were done using the Bruker Simfonia software. Elemental Analyses was performed on a Perkin-Elmer Analyzer 240. Mass spectrometry was carried out on a BRUKER Daltronics Microtof Q mass spectrometer.

Magnetic Characterization. The magnetic susceptibility measurements were performed on solid polycrystalline samples with a Quantum Design MPMS superconducting Quantum Interference Device (SQUID) magnetometer and were all corrected for the diamagnetic contribution as calculated with Pascal's constants. Data were corrected for the magnetism of the sample holder, which was independently determined at the same temperature and fields.

■ ASSOCIATED CONTENT

Supporting Information. Further details are given in Figure S1−S6. This material is available free of charge via the Internet at http://pubs.acs.org.

■ AUTHOR INFORMATION

Corresponding Author
*E-mail: sarkar@iac.uni-stuttgart.de.

■ ACKNOWLEDGMENT

We thank Corinna Schelzel for experimental help and Dr. F. Lissner for crystal measurements. This work was financed by FCI (Chemiefondsstipendium for DS), DFG, SFB-TRR21, the Baden-Württemberg Stiftung, and the Humboldt Stiftung (Sofja Kovalevskaja award of the Bundesministerium für Bildung und Forschung).

■ REFERENCES

(1) (a) Huisgen, R.; Knorr, R.; Möbius, L.; Szeimies, G. *Chem. Ber.* **1965**, *98*, 4014. (b) Huisgen, R.; Szeimies, G.; Möbius, L. *Chem. Ber.* **1967**, *100*, 2492.

(2) (a) Rostovtsev, V. V.; Green, L. G.; Fokin, V. V.; Sharpless, K. B. *Angew. Chem., Int. Ed.* **2002**, *41*, 2596. (b) Tornoe, C. W.; Christensen, C.; Meldal, M. *J. Org. Chem.* **2002**, *67*, 3057. (c) Ahlquist, M.; Fokin, V. V. *Organometallics* **2007**, *26*, 4389. (d) Rodionov, V. O.; Presolski, S. I.; Diaz, D. D.; Fokin, V. V.; Finn, M. G. *J. Am. Chem. Soc.* **2007**, *129*, 12705.

(3) (a) Binder, W. H.; Sachsenhofer, R. *Macromol. Rapid Commun.* **2007**, *28*, 15. (b) Opsteen, J. A.; van Hest, J. C. M. *Chem. Commun.* **2005**, 57. (c) Samanta, D.; Kratz, K.; Zhang, X.; Emrick, T. *Macromolecules* **2008**, *41*, 530.

(4) Kolb, H. C.; Sharpless, K. B. *Drug Discovery Today* **2003**, *8*, 1128.

(5) Evans, R. A. *Aust. J. Chem.* **2007**, *60*, 384.

(6) Wu, P.; Fokin, V. V. *Aldrichimica Acta* **2007**, *40*, 7.

(7) Schweinfurth, D.; Hardcastle, K. I.; Bunz, U. H. F. *Chem. Commun.* **2008**, 2203.

(8) Berlin, M.-A.; Meudtner, R. M.; Demeshko, S.; Meyer, F.; Limberg, C.; Hecht, S. *Chem.—Eur. J.* **2010**, *16*, 10202.

(9) (a) Gispert, J. R. *Coordination Chemistry*; Wiley-VCH: Weinheim, Germany, 2008. (b) Gütlich, P.; Hauser, A.; Spiering, H. *Angew. Chem., Int. Ed. Engl.* **1994**, *33*, 2024.

(10) (a) Carbonera, C.; Dei, A.; Létard, J.-F.; Sangregrorio, C.; Sorace, L. *Angew. Chem., Int. Ed.* **2004**, *43*, 3135. (b) Gütlich, P.; Garcia, Y.; Goodwin, H. A. *Chem. Soc. Rev.* **2000**, *29*, 419. (c) Sato, O.; Cui, A.; Matsuda, R.; Tao, J.; Hayami, S. *Acc. Chem. Res.* **2004**, *40*, 361. (d) Tao, J.; Maruyama, H.; Sato, O. *J. Am. Chem. Soc.* **2006**, *128*, 1790.

(11) Venkataramani, S.; Jana, U.; Dommaschk, M.; Sönnichsen, F. D.; Tuczek, F.; Herges, R. *Science* **2011**, *331*, 445.

(12) (a) Goodwin, H. A. *Top. Curr. Chem.* **2004**, *233*, 59. (b) Gütlich, P.; Goodwin, H. A. *Top. Curr. Chem.* **2004**, *233*, 1.

(13) (a) Goodwin, H. A. *Top. Curr. Chem.* **2004**, *234*, 23. (b) Krivokapic, I.; Zerara, M.; Daku, M. L.; Vargas, A.; Enachescu, C.; Ambrus, C.; Pigot, P. T.; Amstutz, N.; Krausz, E.; Hauser, A. *Coord. Chem. Rev.* **2007**, *251*, 364. (c) Figgins, P. E.; Busch, D. H. *J. Am. Chem. Soc.* **1960**, *82*, 820. (d) Griffith, J. S. *J. Inorg. Nucl. Chem.* **1956**, *2*, 229. (e) Figgins, P. E.; Busch, D. H. *J. Phys. Chem.* **1961**, *65*, 2236. (f) Stoufer, R. C.; Busch, D. H.; Hadley, W. B. *J. Am. Chem. Soc.* **1961**, *83*, 3732. (g) Hogg, R.; Wilkins, R. G. *J. Chem. Soc.* **1962**, 341. (h) Hayami, S.; Shigeyoshi, Y.; Akita, M.; Inoue, K.; Kato, K.; Osaka, K.; Takata, M.; Kawajiri, R.; Mitani, T.; Maeda, Y. *Angew. Chem., Int. Ed.* **2005**, *44*, 4899. (i) Kremer, S.; Henke, W.; Reinen, D. *Inorg. Chem.* **1982**, *21*, 3013. (j) Harris, C. M.; Lockyer, T. N.; Martin, R. L.; Patil, H. R. H.; Sinn, E.; Stewart, I. M. *Aust. J. Chem.* **1969**, *22*, 2105. (k) Judge, J. S.; Baker, W. A. *Inorg. Chim. Acta* **1967**, *1*, 68. (l) Marzilli, L. G.; Marzilli, P. A. *Inorg. Chem.* **1972**, *11*, 457. (m) Hayami, S.; Urakami, D.; Kojima, Y.; Yoshizaki, H.; Yamamoto, Y.; Kato, K.; Fuyuhiro, A.; Kawata, S.; Inoue, K. *Inorg. Chem.* **2010**, *49*, 1428.

(14) (a) Brooker, S.; Plieger, P. G.; Moubaraki, B.; Murray, K. S. *Angew. Chem., Int. Ed.* **1999**, *38*, 408. (b) Beckmann, U.; Brooker, S. *Coord. Chem. Rev.* **2003**, *245*, 17. (c) Brooker, S.; de Geest, D. J.; Kelly, R. J.; Plieger, P. G.; Moubaraki, B.; Murray, K. S.; Jameson, G. B. *Dalton Trans.* **2002**, 2080. (d) Brooker, S. *Eur. J. Inorg. Chem.* **2002**, 2535. (e) Murray, K. S. *Eur. J. Inorg. Chem.* **2008**, 3101.

(15) Li, B.; Tao, J.; Sun, H.-L.; Sato, O.; Huang, R.-B.; Zheng, L.-S. *Chem. Commun.* **2008**, 2269.

(16) (a) Li, Y.; Flood, A. H. *Angew. Chem., Int. Ed.* **2008**, *47*, 2649. (b) Li, Y.; Flood, A. H. *J. Am. Chem. Soc.* **2008**, *130*, 12111. (c) Lee, S.; Hua, Y.; Park, H.; Flood, A. H. *Org. Lett.* **2010**, *12*, 2100. (d) Hua, Y.; Flood, A. H. *J. Am. Chem. Soc.* **2010**, *132*, 12838. (e) Li, Y.; Pink, M.; Karty, J. A.; Flood, A. H. *J. Am. Chem. Soc.* **2008**, *130*, 17293.

(17) (a) Li, Y.; Huffman, J. C.; Flood, A. H. *Chem. Commun.* **2007**, 2692. (b) Struthers, H.; Mindt, T. L.; Schibli, R. *Dalton Trans.* **2010**, *39*, 675. (c) Schweinfurth, D.; Pattacini, R.; Strobel, S.; Sarkar, B. *Dalton Trans.* **2009**, 9291. (d) Donnelly, P. S.; Zanatta, S. D.; Zammit, S. C.; White, J. M.; Williams, S. J. *Chem. Commun.* **2008**, 2459. (e) Schulze, B.; Friebe, C.; Hager, M. D.; Winter, A.; Hoogenboom, R.; Görls, H.; Schubert, U. S. *Dalton Trans.* **2009**, 787. (f) Fletcher, J. T.; Bumgarner, B. J.; Engels, N. D.; Skoglund, D. A. *Organometallics* **2008**, *27*, 5430. (g) Obata, M.; Kitamura, A.; Mori, A.; Kameyama, A.; Czaplewska, J. A.; Tanaka, R.; Kinoshita, I.; Kusumoto, T.; Hashimoto, H.; Harada, M.; Mikata, Y.; Funabiki, T.; Yano, S. *Dalton Trans.* **2008**, 3292. (h) Monkowius, U.; Ritter, S.; König, B.; Zabel, M.; Yersin, H. *Eur. J. Inorg. Chem.* **2007**, 4597. (i) Crowley, J. D.; Gavel, E. L. *Dalton Trans.* **2010**, *39*, 4035. (j) Crowley, J. D.; Bandeen, P. H. *Dalton Trans.* **2010**, *39*, 612. (k) Gower, M. L.; Crowley, J. D. *Dalton Trans.* **2010**, *39*, 2371.

(18) (a) Chen, H.-M.; Shi-Ping, Y.; Chen, Q.-Q.; Zhang, F.; Jia-Min, C.; Yu, X.-B. *Acta Crystallogr.* **2005**, *E61*, m1001. (b) Kirchner, R. M.; Mealli, C.; Bailey, M.; Howe, N.; Torre, L. P.; Wilson, L. J.; Andrews, L. C.; Rose, N. J.; Lingafelter, E. C. *Coord. Chem. Rev.* **1987**, *77*, 89. (c) Gou, S.; You, X.; Yu, K.; Lu, J. *Inorg. Chem.* **1993**, *32*, 1883.

(19) (a) Galet, A.; Gaspar, A. B.; Munõz, M. C.; Real, J. A. *Inorg. Chem.* **2006**, *45*, 4413. (b) Real, J. A.; Gaspar, A. B.; Niel, A.; Munõz, M. C. *Coord. Chem. Rev.* **2003**, *236*, 121. (c) Gaspar, A. B.; Munõz, M. C.; Niel, V.; Real, J. A. *Inorg. Chem.* **2001**, *40*, 9. (d) Jameson, G. N. L.; Werner, F.; Bartel, M.; Absmeier, A.; Reissner, M.; Kitchen, J. A.; Brooker, S.; Caneschi, A.; Carbonera, C.; Létard, J.-F.; Linert, W. *Eur. J. Inorg. Chem.* **2009**, *26*, 3948. (e) Nielsen, P.; Toftlund, H.; Bond, A. D.; Boas, J. F.; Pilbrow, J. R.; Hanson, G. R.; Noble, C.; Riley, M. J.; Neville, S. M.; Moubaraki, B.; Murray, K. S. *Inorg. Chem.* **2009**, *48*, 7033.

(20) Rizzi, A. C.; Brondino, C. D.; Calvo, R.; Baggio, R.; Garland, M. T.; Rapp, R. E. *Inorg. Chem.* **2003**, *42*, 4409.

(21) (a) Chan, T. R.; Hilgraf, R.; Sharpless, K. B.; Fokin, V. V. *Org. Lett.* **2004**, *6*, 2853. (b) Demko, Z. P.; Sharpless, K. B. *Angew. Chem., Int. Ed.* **2002**, *41*, 2110.

(22) Sheldrick, G. M. *SHELXL-97, Program for refinement of crystal structures*; University of Göttingen: Göttingen, Germany, 1997.